Deming Yang
Ming Li*
Chao Lou
Dehao Wan
Yi Yun

Split Heat Pump Distillation Based on Two-Stage Compression for Separating an Acetone-Water Mixture

There is a constant concentration zone for acetone-water mixtures, and the average relative volatility of the two components in the constant concentration zone is only 1.41, so the energy consumption of the conventional distillation process is high. Two kinds of split mechanical vapor recompression (MVR) heat pump distillation processes, i.e., single-stage and two-stage compression processes, were proposed to separate acetone-water mixtures. The thermodynamic data of the mixture were calculated and modules of Aspen Plus were used to simulate the distillation column and steam compressor. Taking the minimum total annual cost as the objective function, the conventional MVR and the two split MVR heat pump distillation processes were simulated and optimized. Compared with the conventional process, the MVR heat pump distillation process had greater economic advantages, and the split heat pump distillation (SHPD) with two-stage compression was superior to the other MVR heat pump distillation processes.

Keywords: Acetone-water mixture, Heat pump distillation, Mechanical vapor recompression, Split heat pump distillation

Received: June 20, 2021; *revised:* October 24, 2021; *accepted:* November 15, 2021

DOI: 10.1002/ceat.202100289

1 Introduction

Under atmospheric pressure, there is a constant concentration zone for acetone-water mixtures. Due to the low relative volatility of the two components in the constant concentration zone, high reflux ratio and high energy consumption are necessary to separate acetone and water by conventional distillation. Therefore, how to reduce the separation energy consumption for acetone-water mixtures with constant concentration zone has attracted increasing attention.

In recent years, more efforts were focused on the energy-saving separation technology [1–4], and a great number of researches were done on the separation of acetone-water at home and abroad. Wang et al. [5] used PVA pervaporation technology to explore the separation of acetone and water. Zhang et al. [6] used the pervaporation technology to separate acetone and water solution by a PDMS composite membrane. Li et al. [7] employed layer-by-layer assembled nanohybrid multilayer membranes to separate acetone aqueous solution. Weires et al. [8] studied acetone recovery by distillation. Ray et al. [9] examined the effect of the type and composition of a copolymer on the separation characteristics for pervaporation of acetone-water mixtures. Wang et al. [10] applied the partition column to the energy-saving research of this system, and found that the total annual cost can be reduced by 41.1 % compared with the conventional distillation process. You et al. [11] used extractive distillation to separate this system. When the purity of acetone reached 99.5 %, the energy can be decreased by 21.9 % and the total annual cost by 16 %.

The distillation process needs a large reflux ratio to separate the two components in the constant concentration zone, but no high reflux ratio is required outside this zone. Based on this characteristic of the mixture, the conventional distillation columns can be divided into upper and lower columns, and different reflux ratio can be used for the two columns. Therefore, the heat pump distillation technology can be applied in the upper or lower column with small temperature difference [12–16], so the split heat pump distillation (SHPD) [17, 18] process is formed.

Zhu et al. [17] researched the economy and operability of SHPD for separating ethanol and water. Yang et al. [18, 19] used SHPD to study the energy-saving effect for 2-methoxyethanol-water and methanol-dimethyl carbonate. Gao et al. [20] used SHPD to investigate the separation of a methanol-chlorobenzene system. The above researches demonstrated that compared with other distillation processes, the SHPD process

Prof. Deming Yang, Ming Li, Chao Lou, Dehao Wan, Yi Yun
wlk_lm@163.com
Changzhou University, Jiangsu Province Advanced Catalysis and Green Manufacturing Collaborative Innovation Center, College of Petrochemical Engineering, Changzhou, 213164, China.

had an obvious energy-saving effect. The SHPD process for separation of acetone and water has not been reported yet.

In this work, the two kinds of SHPD processes with single-stage and two-stage compression are employed to study the energy-saving for separation of acetone-water mixtures with constant concentration zone (pinch point). In particular, the SHPD process with two-stage compression is the first time applied to the energy-saving research for SHPD, i.e., mechanical vapor recompression (MVR) heat pump distillation technology is used for the upper and the lower tower in the SHPD process, respectively, to achieve the maximum energy-saving effect.

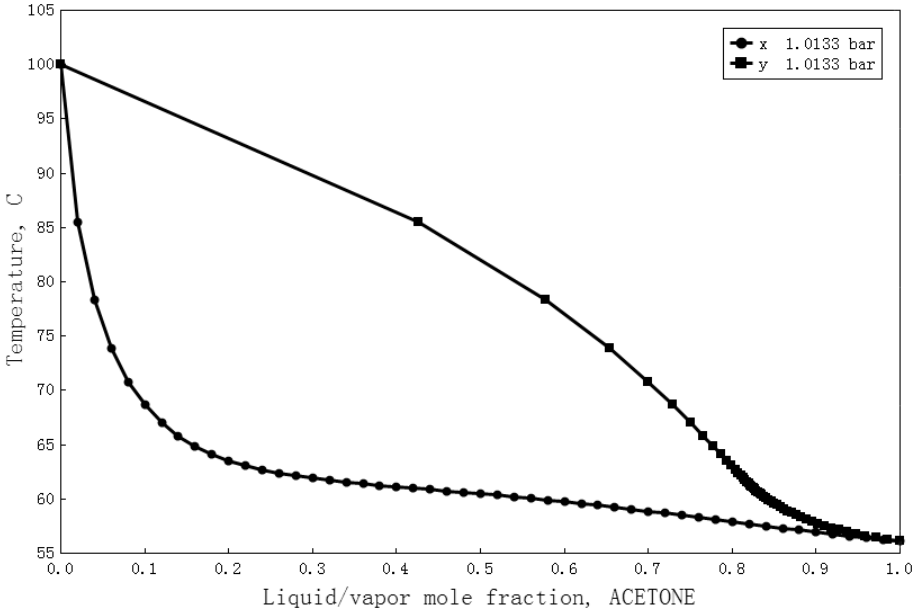

Figure 1. *T-x-y* diagram of acetone-water at atmospheric pressure.

2 Mixture Characteristics

For polar mixture such as acetone and water, the thermodynamic data of the mixture are generally calculated by the activity coefficient equation. The non-random two-liquid Redlich Kwong (NRTL-RK) equation can well describe the constant concentration zone of acetone-water based on the analysis result of a phase diagram (Fig. 1), so this equation was selected to calculate the vapor-liquid equilibrium data of the system. In this equation, the NRTL model was used to calculate the liquid activity coefficient and the Redlich-Kwong (RK) model was taken to determine the gas-phase fugacity coefficient. The binary interaction parameters of the NRTL-RK equation are listed in Tab. 1.

Table 1. Binary interaction parameters of NRTL-RK equation for acetone-water mixture.

i	j	A_{ij}	A_{ji}	B_{ij}	B_{ji}
Acetone	Water	−3.0768	7.9385	1203.73	−2099.67

TBC = 22 688.6 × D1.066 × H0.802

The acetone-water phase equilibrium data calculated by the NRTL-RK equation is depicted in Fig. 1. It can be seen that the mixture of acetone and water belongs to a large temperature difference system with a boiling point difference of about 45 °C, and forms a constant concentration zone in the range of $X_{Acetone}$ = 0.9–1.0 (mole fraction), i.e., the vapor and liquid phase composition is very close, and the average relative volatility is only 1.41 under the constant concentration zone. Outside the constant concentration zone, the average relative volatility is as high as 7.25, therefore, the reflux ratio of distillation varies greatly in the two distillation zones.

In view of the above characteristics of the acetone-water mixture, the conventional distillation column could be divided into upper and lower columns, so a different reflux ratio was used in the two columns. The MVR heat pump technology can be applied in the upper or the lower column with a small temperature difference to significantly reduce the energy consumption of the separation.

3 Evaluation Model

3.1 Total Annual Cost and Standard Coal Consumption

In order to investigate the comprehensive economic benefits of various distillation processes, the total annual cost (TAC) was selected as the evaluation index. Usually, it was composed of two parts, namely, equipment depreciation cost and operation cost. The equipment depreciation cost included the depreciation cost of column body, column internals, compressor, heat exchanger, and other equipment, and the operation cost involved the cost of cooling water, steam, electricity, etc. The calculation formulas of TAC [21] are presented in Tab. 2, where β[1)] is the depreciation life of the equipment and is set at eight years. The annual working hours were set at 7200 h, Q_R and Q_C were the heat load of reboiler and condenser, respectively (GJ h^{-1}), N_T was the number of stages, and 0.28 and 7.72 are the price coefficients of cooling water and steam, respectively, ($ GJ^{-1}).

In order to facilitate the comparison of various energy consumptions, the steam and electricity consumptions were converted into standard coal [22]. The total energy consumption is

1) List of symbols at the end of the paper.

Table 2. TAC calculation formulas.

Category	Formula
Column diameter D [m]	Calculated by ASPEN PLUS software
Column height H [m]	$H = 1.2\times(N_T - 2)\times 0.60$
Column body cost TBC \$	$TBC = 22\,688.6\times D^{1.066}\times H^{0.802}$
Column internals cost TIC \$	$TIC = 1426\times D^{1.55}\times H$
Reboiler exchanger area AR [m^2]	$AR = Q_R/(U_R\times\Delta T_m)$
U_R [kW (°C m^2)$^{-1}$]	$U_R = 0.568$
Condenser exchanger area AC [m^2]	$AC = Q_C/(U_C\times\Delta T_m)$
U_c [kW(°C m^2)$^{-1}$]	$U_c = 0.852$
Heat exchanger cost HEC \$	$HEC = 9445.2\times(AR^{0.65} + AC^{0.65})$
Compressor power PW [kW]	Calculated by ASPEN PLUS software
Compressor cost CPC \$	$CPC = 9476\times PW^{0.62}/7$
Capital cost CC \$	$CC = TBC + TIC + HEC + CPC$
Cooling water cost CWC [\$ yr^{-1}]	$CWC = 0.28\times Q_c\times 7200$
Steam cost SC [\$ yr^{-1}]	$SC = 7.72\times Q_R\times 7200$
Electricity cost EC [\$ yr^{-1}]	$EC = 0.5\times PW\times 7200/7$
Operating cost OC [\$ yr^{-1}]	$OC = CWC + SC + EC$
Total annual cost TAC [\$ yr^{-1}]	$TAC = CC/\beta + OC$

the amount of standard coal consumed. The calculation formulas of standard coal are given in Tab. 3. H_i means the enthalpy of streams (kJ kg^{-1}).

3.2 Thermodynamic Efficiency

Effective energy is a thermodynamic state parameter to characterize the energy level. Strictly speaking, energy-saving means exergy-saving [23]. The thermodynamic efficiency (η) reflects the utilization of effective energy. The greater the loss of effective energy, the lower the thermodynamic efficiency; otherwise, the thermodynamic efficiency is higher. In the MVR heat pump distillation process, because the compressor was used and the electricity consumed by the compressor was all regarded as effective energy, so the actual separation work of the process should include electric energy, and the minimum separation work is the effective energy change of streams. The calculation formulas of thermodynamic efficiency η are presented in Tab. 4.

In Tab. 4, H_i and S_i are the enthalpy and entropy of streams, respectively, (kJ kg^{-1} and kJ $kg^{-1}K^{-1}$), T_0 is the ambient temperature, 273.15 K; PW is the power consumption of the compressor (kW), and T_R and T_C are the temperatures of heating medium and cooling medium, respectively (K).

4 Simulation of Distillation Process

4.1 Basic Data and Simulation Regulations

In the process of waterborne polyurethane production, acetone wastewater is usually obtained. The amount of the acetone wastewater generated is about 5000 kg h^{-1}, the content of acetone is about 0.65 (mass fraction, the same below), and the content of water is 0.35. It is required to separate acetone with a purity not less than 0.998, and the content of acetone in the tower bottom wastewater should be not more than 500 ppm. The Radfrac. module was used to simulate and optimize the distillation column with floating valve tray and the Compr. module to calculate the steam centrifugal compressor. The overhead vapors were cooled by cooling water, inlet temperature and outlet temperature were set at 33 °C and 39 °C, respectively, and the column bottom material were heated by 0.5 MPa saturated steam.

4.2 Conventional Single-Column Distillation Process

The operating pressure of the conventional single-column distillation was set at atmospheric pressure. On the premise of meeting the separation requirements, the sensitivity analysis and design specification module of Aspen Plus software were employed to optimize the theoretical plate, reflux ratio (RR), and feed position based on the principle of minimum TAC. The optimization results showed that the number of theoretical plates was 61, the feed position was at 54 stage, and the reflux ratio was 4.27 as indicated in Figs. 2A and 2B, respectively. The main operating parameters, equipment parameters, and the

Table 3. Standard coal calculation formulas.

Category	Formula
Heating medium consumption HMC [t yr^{-1}]	$HMC = Q_R/H_i\times 3600\times 68/700\times 7200$
Electricity medium consumption EMC [t yr^{-1}]	$EMC = PW\times 7200\times 0.22/700$
Total energy consumption TEC [t yr^{-1}]	$TEC = HMC + EMC$

Table 4. Thermodynamic efficiency calculation formulas.

Category	Formula
Minimum separation work $W_{min,T0}$ [kW]	$W_{min,T_0} = \Delta E = \sum_{out} n_i(H_i - T_0S_i) - \sum_{in} n_j(H_j - T_0S_j)$
Actual separation work $W_{act.}$ [kW]	$W_{act.} = PW + Q_R(1 - T_0/T_R) - Q_c(1 - T_0/T_c)$
Thermodynamic efficiency η [%]	$\eta = W_{min,T0}/W_{act.}$

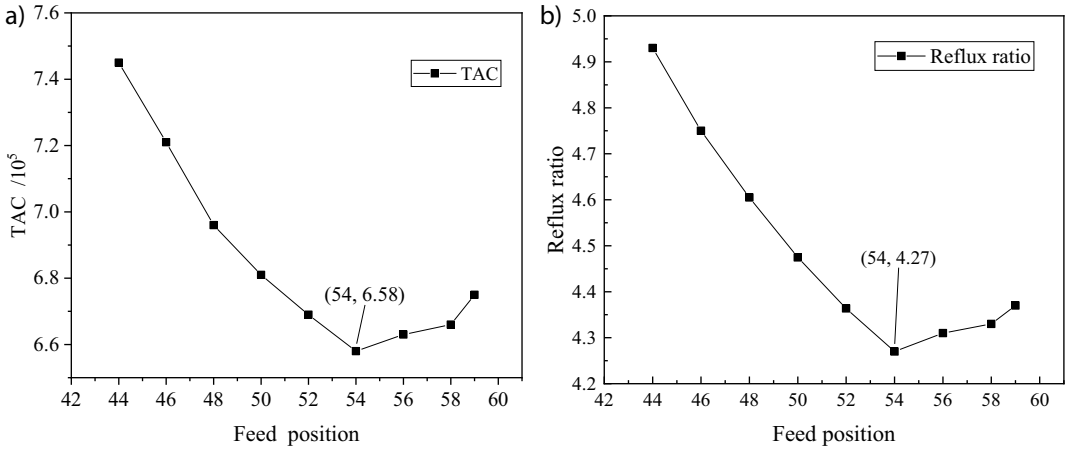

Figure 2. Relationships (A) between feed position and TAC, (B) between feed position and reflux ratio.

temperature distribution in the column are summarized in Fig. 3. Under the above optimized parameters, the energy consumption and TAC of the conventional single-column distillation process were 2311.84 t yr^{-1} standard coal and 6.58×10^5 \$ yr^{-1}, respectively.

4.3 Conventional Single-Column MVR Heat Pump Distillation Process

Fig. 3 illustrates that the heat of overhead vapor was taken away by the cooling water, so large amounts of energy were wasted. In order to make full use of the heat of overhead vapor, the MVR heat pump distillation process as displayed in Fig. 4 was proposed to separate the mixture. The overhead vapor was raised to the desired pressure and temperature through compressor C1 and then used as the heat source for the bottom reboiler E2, and an auxiliary reboiler E3 was added to meet the heat load of the separation process. The heat transfer temperature difference for the bottom reboiler E2 was fixed at 10 °C, then the compression ratio (CR) of C1 was determined by 4.7. When the high-temperature liquid from C1 returned back to T1, it can occur flash evaporation, so a liquid cooler E1 was added to cool the high temperature liquid.

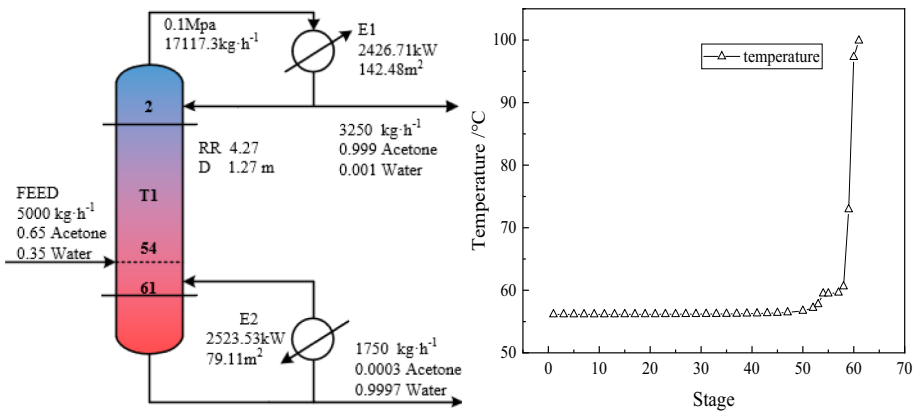

Figure 3. Process flow and optimization results for conventional single-column distillation.

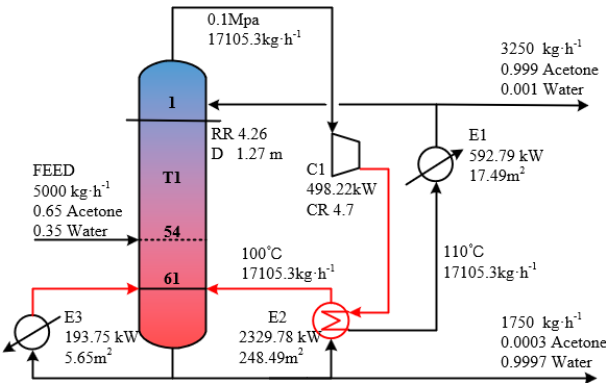

Figure 4. Process flow and results for conventional single-column MVR heat pump distillation.

The main operating parameters and equipment parameters are depicted in Fig. 4. The energy consumption of the conventional single-column MVR heat pump distillation process was the sum of the power consumption of the compressor C1 and the steam consumption of the auxiliary reboiler E3. The energy consumption and TAC of the conventional single-column MVR heat pump distillation process were 1304.91 t yr^{-1} standard coal and 4.95×10^5 \$ yr^{-1}, respectively. Obviously, the conventional single-column MVR heat pump distillation process can save energy and TAC by 43.56 % and 24.77 %, respectively, compared with the conventional single-column distillation process.

As indicated in Fig. 3, the temperature difference between the bottom and top of the column was as high as 43.2 °C, so the compressor C1 needed high CR to meet the heat transfer temperature difference between the top and bottom of the column. As a result, the

power consumption of the compressor C1 increased. To reduce this power consumption, the SHPD process was proposed.

4.4 Split Heat Pump Distillation with Single-Stage Compression Process

Fig. 3 demonstrates that the temperature distribution was flat within the range of less than 53 theoretical plates and suddenly steep within the range of more than 54 theoretical plates. Based on the above temperature distribution characteristic, the column T1 depicted in Fig. 3 was divided into two columns as illustrated in Fig. 5, i.e., the upper column named T1A and the lower column named T1B. Obviously, the constant concentration zone was in the T1A, and the temperature difference between the top and bottom of the T1A was small, so the T1A was suitable for using MVR heat pump distillation technology, that was SHPD with single-stage compression.

As indicated in Fig. 5, part of overhead vapor of the T1A was compressed by the compressor C1 and used as the heat source for the T1A bottom reboiler E2, and part of it mixed with the condensate of the above compressed steam which entered the condenser E1 and condensed by cooling water. Part of the condensate from E1 flowed back into the T1A column as reflux and the rest of it was extracted as acetone product. The stream from the T1A bottom entered the top of the T1B, while the overhead vapor of the T1B returned back to the T1A bottom. The T1B bottom material was heated by fresh steam, and the wastewater was extracted from the T1B bottom. Thus, the energy consumption of the SHPD with single-stage compression was the sum of the power consumption of the compressor C1 and the steam consumption at the T1B bottom.

The MVR heat pump distillation process had the problem of system energy balance [17], while the SHPD process was a special MVR heat pump distillation process, which also suffered from the same issue. The SHPD process is more than simply dividing the distillation column into upper and lower columns, and the determination of the split point was the key of the SHPD process. Usually, the concentration of the liquid phase at the bottom of the upper column, i.e., the concentration of the split point, is used to determine the appropriate split location. In this paper, the purity of acetone in the T1A bottom liquid phase ($X_{Acetone}$) was used as the concentration of the split point.

The split point concentration had a great influence on the equipment cost and operation cost of the whole process. The greater the concentration of the split point, the smaller the temperature difference of the upper column, and the more significant the energy-saving effect of MVR heat pump distillation, so the lower the operating costs of the upper column. But at the same time, the operating load of the lower column will rise, which can increase the operating costs of the lower column. On the contrary, if the concentration of the split point was smaller, the result was opposite to the above. The above analysis demonstrated that there must be an optimal split point concentration for the SHPD process.

The operating parameters and equipment parameters of the upper column and the lower column under different split point concentrations were obtained by Aspen Plus software. Based on the above simulation results, the energy consumption and TAC of the SHPD process were calculated and the summary results are given in Tab. 5. When $X_{Acetone}$ = 0.77, TAC was the smallest, which was 3.76×10^5 \$ yr^{-1}. Therefore, for the SHPD with single-stage compression process, the optimal split point concentration is 0.77. The optimized main process parameters and equipment parameters are summarized in Tab. 5.

4.5 Split Heat Pump Distillation with Two-Stage Compression Process

From the data in Fig. 5 follows that in the SHPD with single-stage compression the total overhead vapor of the T1A was 11403+5320 = 16723 kg h^{-1}, and the vapor entering the compressor was 11 403 kg h^{-1}, so the utilization rate of the overhead vapor was only 68.19 %. Obviously, the overhead vapor of the T1A was not fully utilized, which leads to the loss of energy. In order to make full use of the overhead vapor of the T1A, SHPD with two-stage compression process as illustrated in Fig. 6 was proposed. In the SHPD with two-stage compression, part of the overhead vapor from the T1A was compressed by the compressor C1 and used as the heat source of the T1A bottom

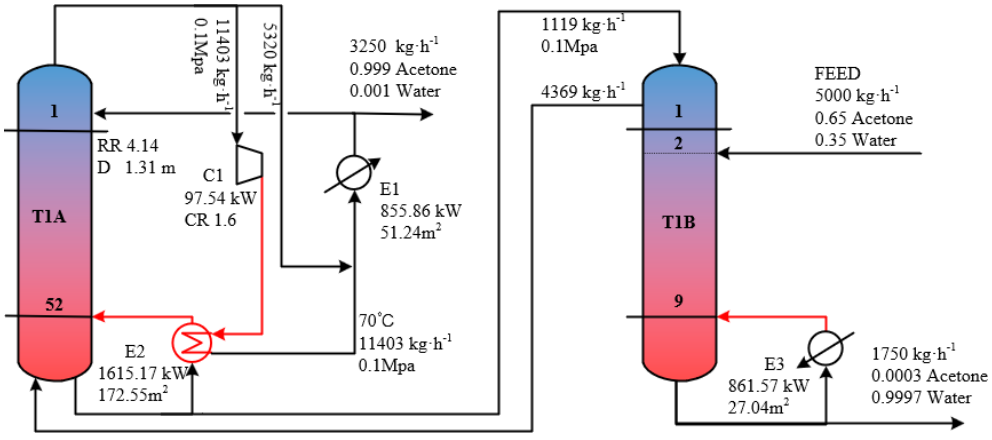

Figure 5. Process flow and optimization results of SHPD with single-stage compression.

Table 5. Summarized simulation results based on different concentration of split points.

$X_{Acetone}$	0.61	0.65	0.77	0.84	0.91
T1A					
stages	56	54	52	50	48
Reflux ratio (*RR*)	4.33	4.28	4.14	4.44	4.47
Compression ratio (*CR*)	1.7	1.7	1.6	1.6	1.5
Column diameter [m]	1.34	1.33	1.31	1.36	1.36
Condenser duty [kW]	775.49	819.44	855.86	917.21	1033.92
Compressor power [kW]	133.68	118.71	97.54	102.36	81.51
T1B					
stages	5	7	9	11	13
Top vapor phase [kg h^{-1}]	3620	3966	4369	4820	5882
Top liquid phase [kg h^{-1}]	5370	5716	1119	1517	2632
Column diameter [m]	0.59	0.65	0.68	0.71	0.77
Reboiler duty [kW]	749.09	797.99	861.57	912.15	1049.67
TAC [\$ yr^{-1}]	3.82×10^5	3.78×10^5	3.76×10^5	3.93×10^5	4.12×10^5

reboiler E2. The rest of it was compressed by the compressor C2 and used as the heat source of the T1B bottom reboiler E3, and an auxiliary reboiler E4 was added to meet the heat load of the separation process.

The condensates from the T1A reboiler and the T1B reboiler entered together the T1A condenser E1 and were cooled by cooling water. Part of the coolant flowed back into the T1A column as reflux and the rest of it was extracted as acetone product. Obviously, the energy consumption of the SHPD with two-stage compression was the sum of the power consumptions of compressor C1 and C2 and the energy consumption of the auxiliary reboiler E4.

Since the SHPD with two-stage compression only employed the unused vapor in the SHPD with single-stage compression, the other operating parameters basically would remain unchanged. Similarly, when the split point concentration $X_{Acetone}$ = 0.77, the minimum value of TAC by simulating was 3.03×10^5 \$ yr$^{-1}\times10^5$. The optimized main process parameters and equipment parameters are summarized in Fig. 6.

4.6 Relationship between Split Point Concentration and Feed Concentration

The split point concentration will change with the change of feed concentration ($X_{Acetone}$). It can be seen from Fig. 1 that the split point concentration will rise with the increase of feed concentration. In order to investigate the effect of different feed concentrations on the split point concentration, by the same research methods as in Sect. 4.4 and based on the principle of minimum TAC, the relationship between the split point concentration and the feed concentration was determined. For the sake of brevity of this manuscript, the calculation process was omitted and only the optimization results are given in Tab. 6. It can be seen from the data in Tab. 6 that the higher the feed concentration, the higher the split point concentration, and when the feed concentration was more closer to the constant concentration zone, the split point concentration was closer to the feed concentration.

Table 6. Optimal split point of different feed compositions.

Feed concentration ($X_{Acetone}$)	0.25	0.40	0.50	0.80
Split point concentration ($X_{Acetone}$)	0.46	0.51	0.65	0.84

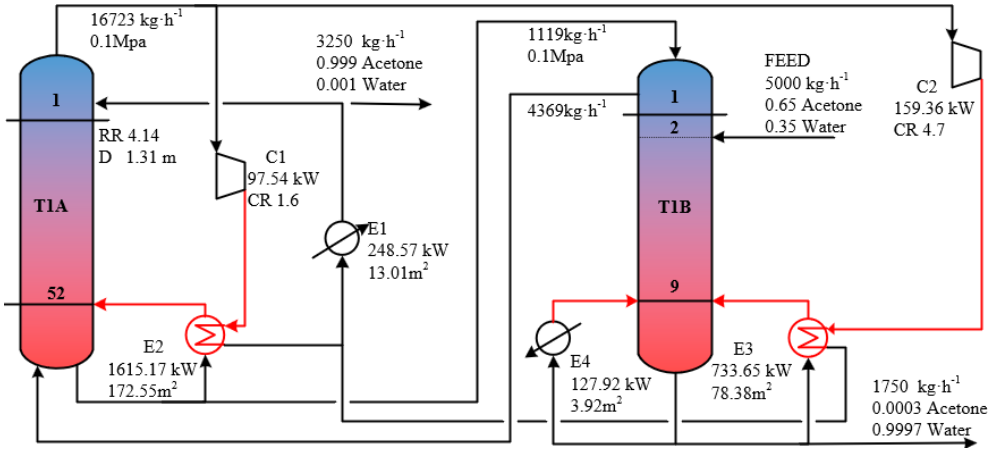

Figure 6. Process flow and optimization results of SHPD with two-stage compression.

5 Comparison of Various Distillation Processes

5.1 Comparison of Thermodynamic Efficiencies

The higher the effective energy utilization rate of the process, the higher its thermodynamic efficiency. Therefore, the effective energy utilization rate can obviously reflect the degree of energy-saving of the distillation process and the irreversible degree of energy conversion [24]. The data obtained by the simulations and optimizations for various heat pump distillation processes were substituted into the calculation formula in Tab. 4, thereby obtaining the thermodynamic data presented in Tab. 7 for various heat pump distillation processes. Because the SHPD with two-stage compression made full use of the overhead vapor, it was 85.62 % and 20.47 % higher than that of the conventional single-column MVR heat pump distillation and the SHPD with single-stage compression respectively.

5.2 Comparison of Main Technical and Economic Indexes

In order to further analyze the energy-saving effect and comprehensive economic benefit for various distillation processes, the main technical and economic indexes from the above simulations were summarized in Tab. 8. The conventional single-column distillation process, conventional single-column MVR heat pump distillation process, SHPD with single-stage compression, and SHPD with two-stage compression were labeled as Scheme I, Scheme II, Scheme III, and Scheme IV, respectively. The data in Tab. 8 indicate that compared with Scheme I, Scheme II can save energy by 43.56 % and TAC by 24.77 %, Scheme III can save energy by 56.31 % and TAC by 42.86 %, and Scheme IV can save energy by 69.78 % and TAC by 53.95 %. It can be concluded that the SHPD with two-stage compression has greater economic advantages in both energy consumption and TAC.

Table 8. Main technical and economic indexes for various distillation processes.

Item	Scheme I	Scheme II	Scheme III	Scheme IV
Standard coal consumption [t yr^{-1}]	2311.84	1304.91	1010.02	698.56
Total capital [\$ yr^{-1}]	1.36×10^5	1.32×10^5	1.47×10^5	1.43×10^5
Operating cost [\$ yr^{-1}]	5.23×10^5	3.63×10^5	2.29×10^5	1.61×10^5
TAC [\$ yr^{-1}]	6.58×10^5	4.95×10^5	3.76×10^5	3.03×10^5
η [%]	5.32	7.23	11.14	13.42
Energy saving [%]	–	43.56	56.31	69.78
TAC saving [%]	–	24.77	42.86	53.95

6 Conclusion

Based on the characteristics of constant concentration zone, the split heat pump distillation process was applied to the separation of acetone and water mixture. The research conclusions are as follows:

- The NRTL-RK equation-of-state can well describe the characteristics of the constant concentration zone for acetone and water mixture, so it is more appropriate to choose it for calculating the vapor-liquid equilibrium data of the mixture.
- For the SHPD process, the optimal concentration of split point is $X_{\text{Acetone}} = 0.77$ when the feed concentration is 0.65.
- When the feed concentration is more closer to the constant concentration zone, the split point concentration is closer to the feed concentration.
- Compared with the conventional single-column distillation process, the conventional single-column MVR heat pump distillation process can save energy by 43.56 % and TAC by 24.77 %, the SHPD with singl-stage compression can save energy by 56.31 % and TAC by 42.86 %, and the SHPD with two-stage compression can save energy by 69.78 % and TAC by 53.95 %, so the latter process has great economic advantages both in energy consumption and TAC.
- The SHPD process provides an effective energy-saving route for separation of mixtures with large temperature difference and constant concentration zone.

The authors have declared no conflict of interest.

Table 7. Thermodynamic efficiency for various heat pump distillation processes.

Item	Conventional single-column MVR heat pump distillation	SHPD with single-stage compression	SHPD with two-stage compression
Condenser duty [kW]	592.79	855.86	284.57
Reboiler duty [kW]	193.75	861.57	127.92
Power consumption of compressor [kW]	498.22	97.54	256.91
$W_{\text{min,T0}}$ [kW]	39.69	39.19	39.19
$W_{\text{act.}}$ [kW]	548.83	351.95	292.08
η [%]	7.23	11.14	13.42

Symbols used

A_{ij},A_{ij}	[–]	parameters of NRTL-RK equation
B_{ij},B_{ij}	[–]	parameters of NRTL-RK equation
AC	[m^2]	condenser exchanger area
AR	[m^2]	reboiler exchanger area
CC	$	capital cost
CPC	$	compressor cost
CWC	[$ yr^{-1}]	cooling water cost
CR	[–]	compression ratio
D	[m]	column diameter
ΔE	[kW]	variable quantity of exergy
EC	[$ yr^{-1}]	electricity cost
EMC	[t yr^{-1}]	electricity medium consumption
H	[m]	column height
HEC	$	heat exchanger cost
H_i	[kJ kg^{-1}]	enthalpy of streams
HMC	[t yr^{-1}]	heating medium consumption
n	[kg h^{-1}]	rate of flow
N_T	[–]	number of stages
OC	[$ yr^{-1}]	operating cost
PW	[kW]	compressor power
Q_C	[GJ h^{-1}]	heat load of condenser
Q_R	[GJ h^{-1}]	heat load of reboiler
RR	[–]	reflux ratio
SC	[$ yr^{-1}]	steam cost
S_i	[kJ $kg^{-1}K^{-1}$]	entropy of streams
T_0	[K]	ambient temperature
TAC	[$ yr^{-1}]	total annual cost
TBC	$	column body cost
T_C	[K]	temperature of cooling medium
TEC	[t yr^{-1}]	total energy consumption
T_R	[K]	temperature of heating medium
ΔT_m	[°C]	log mean temperature difference
U_R,U_C	[kW(°C m^2)$^{-1}$]	heat conveyance coefficient
$W_{act.}$	[kW]	actual separation work
$W_{min,\ T0}$	[kW]	minimum separation work
$X_{Acetone}$	[–]	purity of acetone

Abbreviations

MVR	mechanical vapor recompression
NRTL-RK	non-random two-liquid Redlich Kwong model
SHPD	split heat pump distillation

Greek letters

η	[%]	thermodynamic efficiency
β	[yr]	depreciation life of equipment

References

[1] Y. Kansha, N. Tsuru, K. Sato, C. Fushimi, A. Tsutsumi, *Ind. Eng. Chem. Res.* **2009**, *48 (16)*, 7682–7686. DOI: https://doi.org/10.1021/ie9007419

[2] M. Arjmand, L. Moreno, L. Liu, *Chem. Eng. Technol.* **2011**, *34 (8)*, 1359–1367. DOI: https://doi.org/10.1002/ceat.201000277

[3] M. Errico, G. Tola, M. Mascia, *Appl. Therm. Eng.* **2009**, *29 (8–9)*, 1642–1647. DOI: https://doi.org/10.1016/j.applthermaleng.2008.07.011

[4] G. Kleemann, W. Paul, *Chem. Eng. Technol.* **2010**, *33 (4)*, 603–609. DOI: https://doi.org/10.1002/ceat.200900460

[5] Z. H. Wang, H. L. Li, X. Y. Fan, Y. Gao, *Appl. Chem. Ind.* **2014**, *43 (4)*, 673–676. DOI: https://doi.org/10.16581/j.cnki.issn1671-3206.2014.04.021

[6] Q. Z. Zhang, B. B. Li, P. X. Li, D. Y. Li, P. Yang, D. Sun, *Desalin. Water Treat.* **2016**, *57 (50)*, 23489–23504. DOI: https://doi.org/10.1080/19443994.2015.1137785

[7] J. Li, G. Zhang, S. Ji, N. Wang, W. An, *J. Membr. Sci.* **2012**, *415–416*, 745–757. DOI: https://doi.org/10.1016/j.memsci.2012.05.066

[8] N. A. Weires, A. Johnston, D. L. Warner, M. M. McCormick, K. Hammond, O. M. McDougal, *J. Chem. Educ.* **2011**, *88 (12)*, 1724–1726. DOI: https://doi.org/10.1021/ed2001158

[9] S. Ray, S. K. Ray, *J. Membr. Sci.* **2006**, *270 (1–2)*, 73–87. DOI: https://doi.org/10.1016/j.memsci.2005.06.055

[10] H. H. Wang, J. J. Bian, J. C. Liang, C. L. Li, *Pet. Tech. (China)* **2017**, *46 (2)*, 217–221. DOI: https://doi.org/10.3969/j.issn.1000-8144.2017.02.012

[11] X. Q. You, I. Rodriguez-Donis, V. Gerbaud, *Ind. Eng. Chem. Res.* **2015**, *54 (1)*, 491–501. DOI: https://doi.org/10.1021/ie503973a

[12] C. C. S. Reddy, Y. Fang, G. P. Rangaiah, *Asia-Pac. J. Chem. Eng.* **2014**, *9 (6)*, 905–928. DOI: https://doi.org/10.1002/apj.1842

[13] H. Shahandeh, M. Jafari, N. Kasiri, J. Ivakpour, *Energy* **2015**, *80*, 496–508. DOI: https://doi.org/10.1016/j.energy.2014.12.006

[14] O. Annakou, P. Mizsey, *Heat Recovery Syst. CHP* **1995**, *15 (3)*, 241–247. DOI: https://doi.org/10.1016/0890-4332(95)90008-X

[15] E. Díez, P. Langston, G. Ovejero, M. D. Romero, *Appl. Therm. Eng.* **2009**, *29 (5–6)*, 1216–1223. DOI: https://doi.org/10.1016/j.applthermaleng.2008.06.013

[16] H. Li, Y. Wu, X. Li, X. Gao, *Chem. Eng. Technol.* **2016**, *39 (5)*, 815–833. DOI: https://doi.org/10.1002/ceat.201500656

[17] P. Zhu, X. Feng, *Can. J. Chem. Eng.* **2003**, *81 (5)*, 963–967. DOI: https://doi.org/10.1002/cjce.5450810506

[18] D. M. Yang, Y. Wang, Q. Liao, *Chem. Eng. (China)* **2012**, *40 (5)*, 1–5.

[19] D. M. Yang, Y. Wang, Q. Liao, X. J. Zhang, *Chem. Ind. Eng. Pro. (China)* **2012**, *31 (5)*, 1165–1168. DOI: https://doi.org/10.16085/j.issn.1000-6613.2012.05.031

[20] X. X. Gao, Z. F. Ma, L. M. Yang, J. Q. Ma, *Ind. Eng. Chem. Res.* **2013**, *52 (33)*, 11695–11701. DOI: https://doi.org/10.1021/ie401467r

[21] J. L. Gu, X. Q. You, C. Y. Tao, J. Li, W. F. Shen, J. Li, *Chem. Eng. Res. Des.* **2018**, *133*, 303–313. DOI: https://doi.org/10.1016/j.cherd.2018.03.015

[22] GB/T 50441-2016, *Standard for calculation of energy consumption in petrochemical engineering design*, National Quality Testing Bureau, **2017**.

[23] C. T. Cui, X. G. Li, D. R. Guo, J. S. Sun, *Energy* **2017**, *134*, 193–205. DOI: https://doi.org/10.1016/j.energy.2017.06.031

[24] A. Araujo, R. Brito, L. Vasconcelos, *Energy* **2007**, *32 (7)*, 1185–1193. DOI: https://doi.org/10.1016/j.energy.2006.07.003

